The Canadian Mineralogist
Vol. 36, pp. 563-583 (1998)

COMPOSITION OF COMPLEX LEPIDOLITE-TYPE GRANITIC PEGMATITES AND OF CONSTITUENT COLUMBITE – TANTALITE, CHÈDEVILLE, MASSIF CENTRAL, FRANCE

LOUIS RAIMBAULT[1]

Centre d'Informatique Géologique, Ecole des Mines, 35, rue St-Honoré, F-77305 Fontainebleau Cedex, France and Groupe des Sciences de la Terre, Laboratoire Pierre Süe, C.E.N. Saclay, B.P. 2, F-91191 Gif-sur-Yvette Cedex, France

ABSTRACT

The Chèdeville field of granitic pegmatites extends over *ca.* 1200 m along a SW–NE trend in the southeastern part of the Saint-Sylvestre granite, northern Massif Central, France. The occurrence of lepidolite as the main lithium mineral, and the geochemical characteristics of the pegmatites, enriched in Li, Rb, Cs, Ta, and Sn, point to an affiliation with the rare-element class, complex type, lepidolite subtype. Vein-like pegmatite bodies have a well-developed internal structure, with a coarse upper zone, a fine-grained banded zone, an aplitic zone, and a lower layered zone with vertical wedge-shaped crystals of feldspar. Flow banding is common, and a repetition of the zonation provides evidence of multiple batches of magma. Metasomatism at the margins between units or of enclaves leads to the development of lepidolite-rich rocks. The geochemical characteristics of associated aplites match those of other occurrences of rare-metal granite at several localities in the northern Massif Central. However, Nb–Ta mineral characteristics are different from those of the granitic rocks. Uranmicrolite is restricted to the purple lepidolite zones, and columbite – tantalite is more Mn-rich than in granites. The Mn/(Fe + Mn) value actually varies over a narrow range (±0.01) within each sample, but the variation between different bodies of pegmatite (from 0.90 to 0.96 and 0.99) again suggests multiple intrusions. Metasomatic units (accounting for less than 5% of the bodies) are characterized by a lower Nb/Ta in the whole rock and a higher Mn/Fe in the columbite – tantalite than in corresponding aplitic parts. Such rocks may be strongly enriched in Zr, Hf, and Th, suggesting a significant mobility of these elements at the metasomatic stage.

Keywords: pegmatite field, complex-lepidolite type, LCT group, columbite – tantalite, cassiterite, microlite, metasomatic replacement, bulk-rock chemistry, Chèdeville, Massif Central, France.

SOMMAIRE

Le champ de pegmatites de Chèdeville s'étend sur une longueur d'environ 1200 m, selon une direction SO–NE, dans la partie sud-est du granite de Saint-Sylvestre, Massif Central septentrional, France. La présence de lépidolite comme principal minéral de lithium et les caractéristiques géochimiques des pegmatites, enrichies en Li, Rb, Cs, Ta et Sn, les rattachent à la classe des pegmatites à éléments rares, type complexe, sous-type à lépidolite. Les corps pegmatitiques, formant des veines, ont une structure interne bien développée, avec une zone supérieure grossière, une zone rubanée à grain fin, une zone aplitique, et une zone litée inférieure avec des cristaux de feldspath pointant vers le haut. Les textures fluidales sont courantes, et des duplications de la zonalité montrent qu'il s'agit d'intrusions multiples. Une métasomatose aux limites entre zones ou sur des enclaves conduit à la formation de roches violacées contenant des concentrations de lépidolite. Les caractéristiques géochimiques des parties aplitiques ressemblent à celles d'autres granites à métaux rares connus dans plusieurs localités du nord du Massif Central. Cependant, les caractéristiques des minéraux de Nb–Ta sont différentes de celles des minéraux de granite. L'uranmicrolite ne se trouve en abondance que dans les unités violacées à lépidolite, et la columbite – tantalite est plus riche en Mn que dans les granites. Dans chaque échantillon, le rapport Mn/(Fe + Mn) ne varie que dans un intervalle restreint (±0.01), mais est variable d'un échantillon à l'autre, nouvelle indication des intrusions multiples, avec Mn/(Fe + Mn) variant de 0.90 à 0.96 et 0.99. Les unités métasomatiques, représentant moins de 5% des corps pegmatitiques, ont des rapports Nb/Ta en roche totale inférieurs, et Mn/Fe dans la columbite – tantalite supérieurs, à ceux des unités aplitiques correspondantes. Ces unités peuvent être fortement enrichies en Zr, Hf et Th, témoignant ainsi d'une forte mobilité de ces éléments au stade métasomatique.

Mot-clés: champ de pegmatites, type complexe à lépidolite, groupe LCT, columbite – tantalite, cassitérite, microlite, remplacement métasomatique, chimie en roche totale, Chèdeville, Massif Central, France.

INTRODUCTION

A rare-metal belt runs over more than 100 km through the northern French Massif Central [*e.g.*, Burnol (1974), Cuney & Raimbault (1991), and references therein]. Among the four major occurrences of Ta–Li–Sn mineralization that constitute the belt, two are albite – lepidolite granite bodies at Beauvoir and Montebras, a third is a rhyolite dyke at Richemont, and a fourth is the Chèdeville granitic pegmatite field,

---

[1] *E-mail address*: raimbault@cig.ensmp.fr

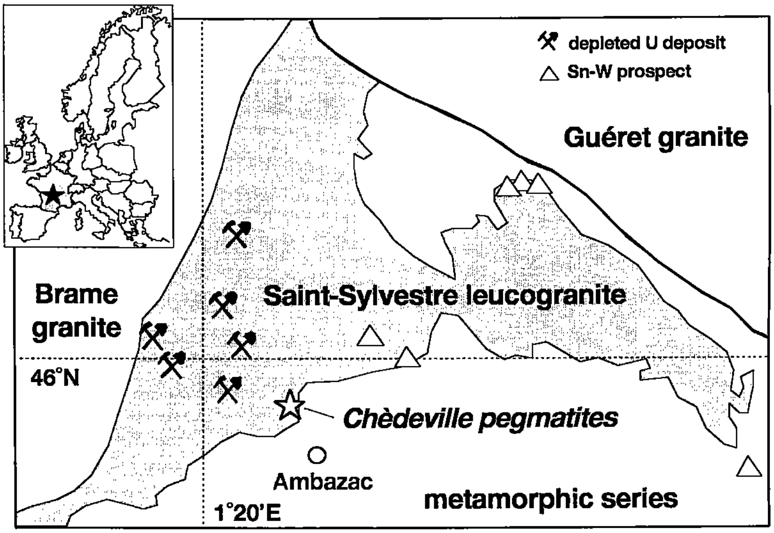

FIG. 1. Location of the Chèdeville pegmatite field in the Saint-Sylvestre massif, northern Massif Central, France. Geological boundaries after Chantraine *et al.* (1974b).

a member of the Haute-Vienne granitic pegmatite district (pegmatite field and district are here used according to the definition given by Černý 1982). The Beauvoir granite is presently mined for china clay, and cassiterite and niobates – tantalates are recovered as by-products. The Montebras granite is mined for albite, but its marginal pegmatitic facies ("stockscheider") and quartz cap ("quartzglocke") have been mined for tin in the nineteenth century. Finally, the Chèdeville granitic pegmatites have been exploited for Li in small quarries and short galleries from 1929 to 1938 (Sarcia 1957).

Precise ^{39}Ar/^{40}Ar dating yields a common age for the four occurrences (Cheilletz *et al.* 1992; pers. commun.), reinforcing the case for a single magmatic episode. The occurrence of rare-metal-enriched rocks as either granite cupolas, subvolcanic dykes or pegmatite veins raises the question as to why the crystallization of these melts resulted in such textural differences. The aim of this paper is to provide a detailed geochemical and mineralogical study of the Chèdeville pegmatites, allowing comparison with the extensive data set obtained on the Beauvoir granite using the same methods (Raimbault *et al.* 1995, and references therein).

GEOLOGICAL SETTING

Regional setting

The Chèdeville pegmatite field is located in the easternmost part of the Haute-Vienne pegmatite district, whose extension coincides roughly with the central part of a granitic batholith (Fig. 1). An east–west section of this batholith grades from the deepest parts in the Brame unit, to intermediate levels in the Saint-Sylvestre unit *sensu stricto*, and to the top of the pluton in the Saint-Goussaud unit. The main facies is a coarse-grained porphyritic two-mica granite, which is intruded, in the Brame and Saint-Sylvestre units, by fine-grained two-mica granites. The batholith is intrusive into a high-grade gneissic series, consisting of meta-sedimentary and meta-igneous rocks.

Whereas the Brame unit is barren, the two other units are associated with various metallic concentrations (Chantraine *et al.* 1974a). Late-magmatic hydrothermal activity resulted in uneconomic Sn–W-bearing quartz veins scattered at the periphery of the Saint-Goussaud two-mica granite, at the roof of the pluton. Late- to post-Hercynian circulation of a hydrothermal fluid are responsible for numerous uranium-bearing veins and episyenites of the La Crouzille ore district, which were intensely exploited until recently. Lenses of beryl-bearing pegmatite have been exploited for feldspar in the last century around Chanteloube, at the northeastern edge of the uranium district. The Chèdeville lithium-bearing pegmatite veins are distributed on either side of the contact between the granite and the surrounding gneisses.

Porphyritic granites have been dated at 324 ± 4 Ma using the U–Pb method on zircon and monazite in the Brame unit (Holliger *et al.* 1986) and at 326 ± 18 Ma using the Rb–Sr method in the Saint-Sylvestre unit (Duthou *et al.* 1984). On the other hand, lepidolite from the Chèdeville pegmatites has been dated at

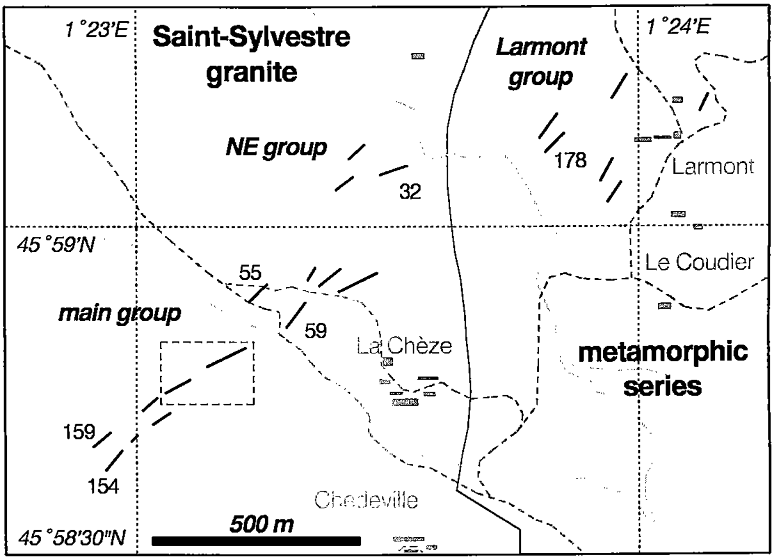

Fig. 2. Geological sketch map of the Chèdeville pegmatite field. Limits of the granite massif after Chantraine *et al.* (1974b). The observed pegmatite bodies, represented by the thick lines, are indicated by sample numbers; the square in the Main group outlines the area of Figure 3.

309 ± 0.9 Ma by the ^{39}Ar/^{40}Ar method (Cheilletz *et al.* 1992). Although a comparison of ages determined by different isotopic systems may be risky, confidence in the reality of the age difference is raised by the case of the very similar Beauvoir granite at Echassières, where different methods of dating yielded identical results (Raimbault *et al.* 1995). So, if the ^{39}Ar/^{40}Ar age records the primary cooling of the pegmatite, it points to a *ca.* 16 Ma gap between emplacement of the porphyritic granite and intrusion of the pegmatite-forming melts, precluding the Saint-Sylvestre two-mica granite as a possible parent for the pegmatite-forming melts. The Les-Sagnes muscovite granite body outcrops about 2 km to the northeast of the Chèdeville field. Although its age is at present unknown, the latter granite has a distinctly sodic character and could represent a member of the parental suite of granites of the pegmatite (M. Cuney, pers. commun.).

Internal structure of the pegmatite field

The pegmatite field is subdivided into several pegmatite groups according to the geographical distribution of dyke swarms and to the surrounding rocks. The Larmont and Vieux groups, located at the northeastern edge of the field, occur as lenses intrusive into metamorphic rocks, whereas all other groups are intrusive into the porphyritic two-mica granite. In the central part of the field (Fig. 2) are the Chèdeville *s.s.* and La Chèze groups, which will be referred to as the main group in the following. In the same area, the northeastern group is distinguished from the previous ones because of an apparent geometrical gap. The Puy-Garsault and Puy-Bertrand groups are located a few km to the southwest of the main group (Sarcia 1957), and are not considered in this study.

Although small quarries provide good outcrops for the largest veins of pegmatite, especially in the main group, there are no outcrops between the quarries, so that the overall shape of the pegmatite bodies must be inferred. As a rule, the pegmatites occur as veins with sharp contacts with surrounding rocks. The width of the veins ranges from 40 cm in the gneisses to about 3 m for the largest veins cutting the granite, where several veins may run parallel a few meters from each other. The vein swarm has been interpreted as very regular parallel veins running over more than 700 m (Sarcia 1957). In this interpretation, dashes representing pegmatite veins on Figure 2 must be connected to form a continuous line. However, a detailed mapping of the best exposed part of the veins (Fig. 3) argues for the existence of discontinuities between different vein-like bodies.

Whereas the dip of the veins is almost constant around 45°, their direction is clearly bimodal in the main group, clustering around two values at N64 ± 2° and N37 ± 4°. The switch between the two directions is very sharp, and the projection of the two sets of veins

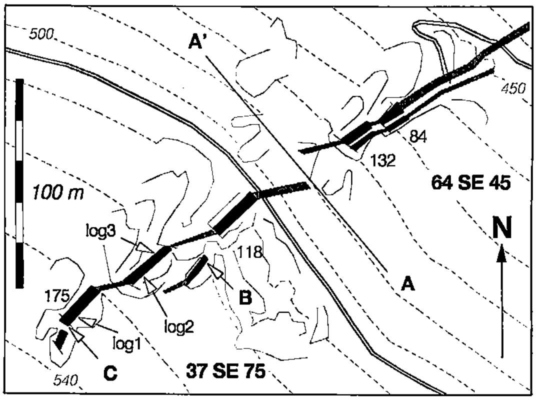

FIG. 3. Detailed map of small quarries in the central part of the Main group, Chèdeville pegmatite field. Observed pegmatite bodies in black, inferred pegmatites in grey areas (kinks are due to projection effects), access tracks and contour lines (in m) in grey lines. Line A–A', trace of the vertical projection plane of Figure 4; points B and C are described in text. Numbers refer to samples of the "lch" series. Labels "log" give the location of sections of Figure 5. Orientation and dip of veins in the two domains are indicated in bold.

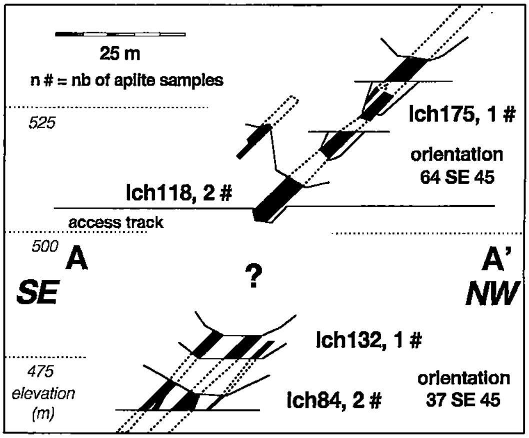

FIG. 4. Projection of pegmatite bodies on vertical plane A–A' (see Fig. 3), equivalent to an idealized view of pegmatite outcrops on the hillslope, with a horizontal line of sight from the northeast, perpendicular to plane A–A'. This is not a cross-section of the pegmatite swarm, since there are hints that a discontinuity occurs at the location of the question mark (see text).

on a perpendicular plane A–A′ at the transition point (Fig. 4) shows that a discontinuity does occur. A fault is an unlikely explanation because (1) it would have to be a large fault in order to change so dramatically the strike of the veins, and in this case it is difficult to accept that, by chance, the two parts of the vein swarm almost match, and (2) there are barren prospecting trenches between the two zones of outcrop. Instead, the case for distinct very flat box-shaped bodies is supported by several facts. (1) In places (B and C in Fig. 3), one can observe sharp (but unfaulted) terminations of veins along fractures apparently conjugate to the main contact surfaces. (2) The width of a single body may vary over short distances (log2 and log3, Fig. 5), and the widening is due to small step-like features that use the same system of fractures as above. (3) The configuration of the dyke swarm is very different on both sides of the A–A′ line at the 490 m level (Fig. 4).

The most convenient way to reconcile all these features is to represent the pegmatite field as a group of flat vein-like boxes with a narrow thickness (less than 4 m), a restricted horizontal extent (less than 100 m and in some cases much less), and a large extent along the dip, with some digitations (Fig. 4). In this way, one can imagine the emplacement of the Chèdeville pegmatites in a pull-apart system resulting from brittle tectonic events. The surrounding granite must have been "cool" at that time, in agreement with the relative ages of the rocks.

STRUCTURE AND COMPOSITION OF THE PEGMATITE VEINS

Organization of the different units

In the main group, the internal structure of the veins is somewhat constant and strongly asymmetrical (Fig. 5). Schematically, each vein is layered and built up of four main units, which are, from the roof to the wall, a coarse albite-rich zone, a banded aplite zone, a massive aplite zone, and a layered aplite zone. The latter zone differs from the massive aplite zone by the presence of thin, light-colored, quartz-rich bands on which upwardly oriented crystals of K-feldspar are rooted. A thin (less than 10 cm) aplitic border-zone is always present at the wall. The structure of the pegmatite veins seems very similar to the structure of the layered lower portion of the Himalaya pocket pegmatite, as described by Foord (1976).

This simple structure is perturbed in several ways. 1) At places, zoning is duplicated (see log 3, Fig. 5), implying a re-opening of the veins after a first batch of melt was emplaced. 2) Large crystals of K-feldspar are dispersed throughout the upper coarse zone; locally, they may account for more than 75% of the rock, defining a "blocky K-feldspar unit" which is a potassium-rich analog of the coarse albite zone. 3) The coarse albite-rich zone is locally cut by thick veins (more than 5 cm wide) of the same material, and aplitic

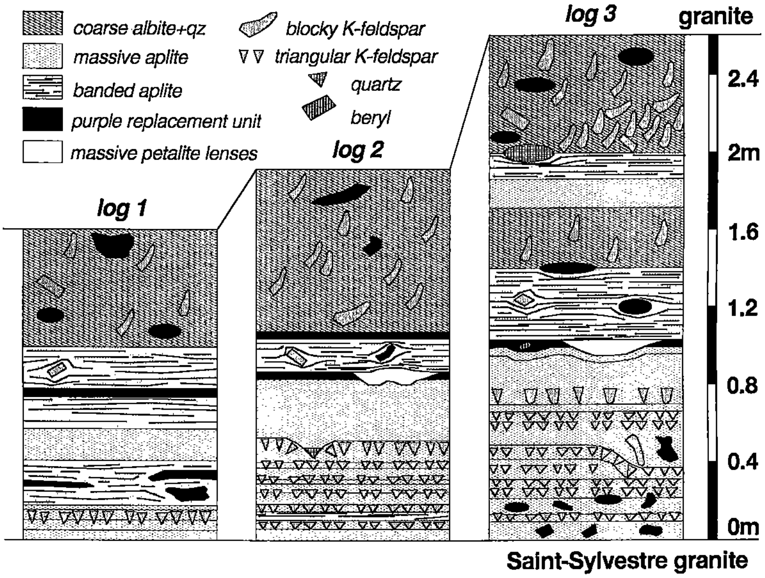

FIG. 5. Typical detailed "stratigraphic" logs across a pegmatite body of the Main group (location on Fig. 3). Upward pointing triangles are K-feldspar crystals. See text for details.

units are locally cut by thin veins, about 1 cm wide, of other aplitic rocks. 4) Purple rocks consisting mainly of lepidolite and quartz ("massive lepidolite unit") are present either as angular or rounded inclusions in other zones. 5) Very regular thin layers of pink to light purple rocks, a few cm wide, may occur at the contact between units. These "lepidolite layers" are continuous over tens of meters, but are in some cases interrupted by creamy white, concave-downward monomineralic lenses of massive petalite, the occurrence of which indicates the low-pressure conditions of crystallization of the pegmatites (London 1984). 6) Small blocks of quartz may be occasionally found between the coarse and banded aplite zones.

Oriented K-feldspar crystals are common in the coarse zone at the roof and in the layered aplite zone at the wall of the pegmatite veins. Their roughly triangular and, in some cases, incurved shape indicates unambiguously that crystallization proceeded inward in the two zones. No time constraint can be proposed for the two zones. Several observations imply that the successive layers in the layered aplite zone were already partly solid but still very plastic, whereas the next layer was still liquid. First, the surface of successive layers is exactly the same shape, although irregular in three dimensions, as the surface of the previous layer. In addition, in places the upper surface of a layer is deformed by the fall of an angular block of quartz that sank through the melt of the next layer (Fig. 5, log 2). Banding in the banded aplite zone is related to variations in relative abundance of the major minerals quartz and mica. The texture is very similar to that of flow-banded rhyolites (*e.g.*, Lentz 1997), suggesting a viscous flow in a low-viscosity melt carrying various inclusions of large crystals of feldspar or fragments of the massive lepidolite unit. The lepidolite layers occurring at the contacts between zones appear as reaction products resulting from the exsolution of fluids from one of the zones.

The preceding observations indicate that melt injection and crystallization are simultaneous. A dynamic interpretation of the rhythmic aspect of the layered zone involves a series of pulses of the same melt, each pulse adding a new layer to the stack of the existing ones. There was no time gap between the different pulses, since a previously emplaced melt was not yet consolidated when the next one arrived. In this context, the massive aplite zone located at the top of the layered aplite zone may be interpreted as a last pulse of melt of larger volume. The banded aplite zone may therefore represent the last pulse of magma in the sequence.

On the other hand, a purely dynamic mode of emplacement is hard to reconcile with the occurrence of very thin layers. As an alternative, the layering could result from *in situ* oscillatory nucleation in the melt after emplacement. The two models could also be combined, with oscillatory nucleation processes being enhanced by melt flow. Strong evidence for concomitant crystallization and emplacement in the shallow

TABLE 1. MINERALOGICAL COMPOSITION OF UNITS CONSTITUTING THE PEGMATITE VEINS

	aplite units			coarse pegmatite	lepidolite bodies (massive)	(layers)
	NE group	Larmont	main group	main group		
albite	A	A	A	A	()	()
quartz	A	A	A	A	A	A
K-feldspar	C	C	C	F	()	()
petalite						R
lepidolite			C	C	A	A
muscovite	C	C	C	C	A	A
topaz	F		F	C	C	C
beryl				L		R
bertrandite			VR			
zircon	VR		VR	L	R	R
amblygonite		R	F	C	C	()
montebrasite				F		
apatite		R	R	F		
monazite	VR					
cassiterite	C	C	C	C	C	C
columbite-tantalite		C	F	C	C	
ixiolite			R			
tungstenian columbite		R				
microlite					F	
uranmicrolite			R	L	C	C
uraninite	R		VR			
niobian rutile	VR					

A, abundant (*i.e.*, major rock-forming mineral); C, common (*i.e.*, present in every thin section); F, common but may be absent in some samples; R, rare; VR, very rare; (), relics of previous stages; L, mineral described by Lacroix (1893, 1901, 1910). Low-temperature alteration phases are excluded from this Table.

Chèdeville pegmatite veins is at odds with the model derived by London (1992) for the one-time emplacement of large volumes of pegmatite-forming melt as confined bodies in deep-seated terranes. It could be viewed as a pulse-like variant to the proposal of a continuous drain from a layered chamber, as described in the Pegli and Buck dykes, Bernic Lake, Manitoba (Černý & Lenton 1995).

Petrography of facies

A short description of the mineralogical composition of the various units is given in Table 1. This study focused primarily on the massive aplite units and their metasomatic alterations; thus the petrography of the coarse zone will not be described in detail. Estimates of the abundances of minerals result from a combination of visual estimates in thin section, and an evaluation using major-element composition.

At the magmatic stage, the major rock-forming minerals in aplite units of the main group are albite (35–45 vol.%), quartz (25–30%) and muscovite – lepidolite mica (12–25%). Lepidolite accounts for roughly 40% of the total mica content. K-feldspar is subordinate (5–10%). Accessory minerals include topaz (5%) and amblygonite (1–2%). Aplite units in the northeastern and Larmont groups are distinctly richer in albite (50 and 60%, respectively) and correspondingly poorer in mica (about 6%), K-feldspar (4%), and topaz (2–3%).

In aplite units of the main group, idiomorphic inclusions of muscovite in quartz crystallize early in the paragenetic sequence. On the other hand, the abundance of muscovite and lepidolite increases dramatically in some samples of pink aplite as the result of greisen-like metasomatic alteration. However, in aplite samples devoid of the greisen stage of alteration, it is not uncommon to observe muscovite cores surrounded by a lepidolite rim, showing that crystallization of lepidolite started at the magmatic stage and lasted up to the metasomatic stages. This observation also suggests that lepidolite saturation in the melt was achieved only late in the crystallization sequence, in agreement with similar observations on rare-metal-bearing volcanic rocks (Raimbault & Burnol 1998) and microgranites (Charoy & Noronha 1996).

The assemblages of accessory minerals are distinct in the different pegmatite groups. In aplite units of the main group, xenomorphic cassiterite and idiomorphic columbite – tantalite crystals are very common. Ixiolite is rare, occurring either as independent crystals or as a rim around tantalite crystals. Xenomorphic apatite is an alteration product of amblygonite or of feldspars, which are P-rich in similar parageneses (London *et al.* 1990). Tiny metamict minerals include uranmicrolite and, less commonly, zircon. Despite the high Be contents of the whole rocks, beryllium minerals are very rare; bertrandite has been identified in small miaroles only. The same problem concerning the location of Be has been observed in the Beauvoir granite (Wang *et al.* 1992b). The accessory-mineral paragenesis of the Larmont group is similar but less evolved; microlite and ixiolite are absent, and small needle-like crystals of tungstenian columbite are found as inclusions in quartz and topaz, as described under the name "wolframoixiolite" in the Phuket pegmatites by Suwimonprecha *et al.* (1995). In contrast, the northeastern group has a rather different assemblage, with monazite and uraninite as carriers of U instead of uranmicrolite, and niobian rutile as carriers of Nb–Ta instead of columbite.

Three types of metasomatic alteration have been identified. In the first, topaz and, in part, mica, are replaced by K-feldspar, with conservation of the aplitic texture of the rock. This change has been observed in one sample around K-feldspar veinlets containing idiomorphic apatite at the wall, rare disseminated uraninite, and vuggy apatite at the center. Secondly, lepidolite-layer units are characterized by intense silicification and development of mica, with quartz and mica accounting each for 45 wt% of the rock. About 20 wt% of the mica is lepidolite. Albite, K-feldspar, and amblygonite occur as relics only, and beryl has been observed in outcrop. Nb and Ta are carried by cassiterite and uranmicrolite. In the associated massive petalite lenses, quartz, albite, topaz and lepidolite occur only in veinlets. Thirdly, the formation of massive lepidolite units starts with the development of numerous crystallites of mica. At this stage, the aplitic texture is still preserved, and the rock takes a light purple-red color. Chemical alteration seems limited, however, since such samples of aplite do not behave anomalously (see below). With the progress of the reaction, the aspect of the rock changes drastically, and quartz and mica make up 40% of the rock each. Despite the similarity with the previous case, this stage is characterized by conservation of the ratio of lepidolite to total mica, and by presence of amblygonite and columbite – tantalite. The latter mineral may be surrounded by microlite; zircon is locally abundant.

The petrographic characteristics of the Chèdeville pegmatites relate them unambiguously to the complex type, lepidolite subtype in the classification of rare-element pegmatites by Černý (1989, 1992). They represent, however, an unusual class in this subtype, owing to a noticeable amount of phosphorus, present as amblygonite, which links them to the P-rich class of Ta-bearing granites (Raimbault *et al.* 1991).

MINERALOGY OF THE RARE-ELEMENT PEGMATITES

Columbite – tantalite group

Columbite – tantalite is the most common Nb–Ta mineral (Table 2). Chemical evolution in the columbite – tantalite quadrilateral shows very distinct populations for the northeastern, Larmont and main groups (Fig. 6a). In the Northeastern group, the Nb–Ta carrier is niobian rutile, with Nb predominant over Ta and a Mn/Fe ratio close to 0. The Larmont group is characterized by two clusters, a first one with low X_{Ta} [defined as the atomic ratio Ta/(Nb + Ta)] constituted by needle-like tungstenian columbite inclusions in quartz and topaz, and the second one with $X_{\mathrm{Ta}} \approx 0.5$ constituted by columbite crystals. Both have intermediate X_{Mn}, very different from the values encountered in the main group.

TABLE 2. COMPOSITION OF COLUMBITE – TANTALITE AND RELATED MINERALS, CHEDEVILLE, MASSIF CENTRAL

group	main group				
unit	coarse pegmatite		aplite units		
sample	lch176d		lch154	lch82e	lch118b
spot #	5818	5824	5780	238	5625
$\mathrm{WO_3}$	0.95	5.66	3.77	0.74	0.43
$\mathrm{Nb_2O_5}$	54.79	59.00	63.99	56.38	21.00
$\mathrm{Ta_2O_5}$	23.54	12.25	9.75	25.22	61.93
$\mathrm{TiO_2}$	0.46	2.63	1.93		0.19
$\mathrm{SnO_2}$			0.42	0.25	0.59
$\mathrm{Sc_2O_3}$	1.30				
FeO	1.37	2.29	2.00	0.29	0.30
MnO	17.89	17.39	17.37	17.89	14.97
total	100.30	99.22	99.23	100.77	99.41
W	0.015	0.088	0.058	0.012	0.008
Nb	1.527	1.600	1.710	1.576	0.713
Ta	0.395	0.200	0.157	0.424	1.265
Ti	0.021	0.119	0.086		0.011
Sn			0.010	0.006	0.018
Sc	0.070				
Fe	0.071	0.115	0.099	0.015	0.019
Mn	0.934	0.884	0.870	0.937	0.953
A site	1.075	0.999	0.969	0.952	0.972
B site	1.958	2.007	2.021	2.018	2.015

group	main group			Larmont	NE group
unit	aplite	massive lepidolite		aplite	aplite
sample	lch154	lch84c	lch171	lch178	lch32
spot #	6242	6315	442	5861	5560
	ixiolite			tung. col.	rutile
$\mathrm{WO_3}$		1.93	0.86	19.71	0.41
$\mathrm{Nb_2O_5}$	6.93	53.53	38.19	41.64	3.85
$\mathrm{Ta_2O_5}$	64.20	27.03	43.43	16.05	1.17
$\mathrm{TiO_2}$	0.38	0.15		0.99	83.04
$\mathrm{SnO_2}$	16.10	0.24	0.75	1.03	
$\mathrm{Sc_2O_3}$					
FeO	0.49	0.17		11.71	8.38
MnO	11.29	17.45	16.20	8.34	
total	99.39	100.50	99.46	99.47	96.85
W		0.031	0.015	0.331	0.005
Nb	0.251	1.517	1.181	1.222	0.076
Ta	1.399	0.461	0.808	0.283	0.014
Ti	0.023	0.007		0.048	2.728
Sn	0.515	0.006	0.020	0.027	
Sc					
Fe	0.033	0.009		0.635	0.306
Mn	0.766	0.927	0.939	0.458	
A site	0.799	0.936	0.939	1.093	
B site	2.188	2.022	2.024	1.911	

"tung. col." stands for tungstenian columbite.
Structural formulæ on the basis of 6 oxygen atoms per formula unit.
A blank indicates values below detection limits: $\mathrm{WO_3}$, 0.08%; $\mathrm{TiO_2}$, 0.05%; $\mathrm{SnO_2}$, 0.04%; $\mathrm{Sc_2O_3}$, 0.08%; FeO, 0.03%.

In contrast, columbite – tantalite of the main group is characterized by a continuous trend from manganocolumbite to manganotantalite, quite in agreement with the trends defined for columbite – tantalite in the lepidolite subgroup of pegmatites by Černý (1989). The enlargement of the Mn-rich part of the quadrilateral (Fig. 6b) shows that the "trend" actually looks like a two-dimensional field. Individually, however, each body of aplite defines a narrow trend (Fig. 6c) beginning with a “horizontal” branch at constant X_{Ta}, a short arcuate segment, and a “vertical” branch at X_{Mn} constant. Only a few aberrant compositions exist. Ixiolite rims on columbite – tantalite display the same trend. One independent grain of ixiolite is, however, discordant. When applied to all samples, the approach resolves the two-dimensional field into several lines, with a common initial X_{Ta} and discrete “asymptotic” X_{Mn} values, each of which is characteristic of one sample or group of samples (Fig. 6d).

Whether the “asymptotic $X_{\mathrm{Mn}}^{\mathrm{cbta}}$” parameter is significant with regard to the history of the host rock has been tested by comparing it to the X_{Mn} ratio in whole rock (Fig. 7). Aplite bodies define a tight correlation, with the exception of three samples. Among these, an incipient development of mica is observed in two samples (118a and 55), and the third one is modified by development of K-feldspar (see above). Sample 154, in which mica development is less noticeable but present, also lies above the correlation line. In contrast, the bodies of lepidolite have high X_{Mn} values in both whole-rock and columbite – tantalite.

A combined interpretation of Figures 6 and 7 leads to the following scenario: 1) In the horizontal branch, magmatic evolution is dominated by changes in Fe/Mn due to precipitation of Fe-bearing minerals, whereas Nb/Ta remains almost constant because columbite – tantalite has just begun to precipitate. Since the different bodies of granitic pegmatite have almost identical Nb/Ta values, X_{Ta} values coincide. 2) As columbite – tantalite crystallizes, a large scatter of X_{Ta} results, whereas X_{Mn} is buffered at a constant value, characteristic of the initial Fe/Mn of the melt. Samples from the same quarry bear identical Fe/Mn fingerprints, suggesting identical sources for the corresponding melts. 3) Some samples underwent metasomatic alteration; thus the X_{Mn} values of columbite – tantalite are reset at higher values, whereas the effect on the much more abundant Fe–Mn-bearing minerals (and hence on whole rocks) is negligible, leading to a departure from the initial trend. 4) Once metasomatic changes were almost complete, the Fe/Mn values of the rocks also were reset at high values. Resetting of Fe/Mn is explained by different partitioning behavior of Fe and Mn between melt and exsolved fluids.

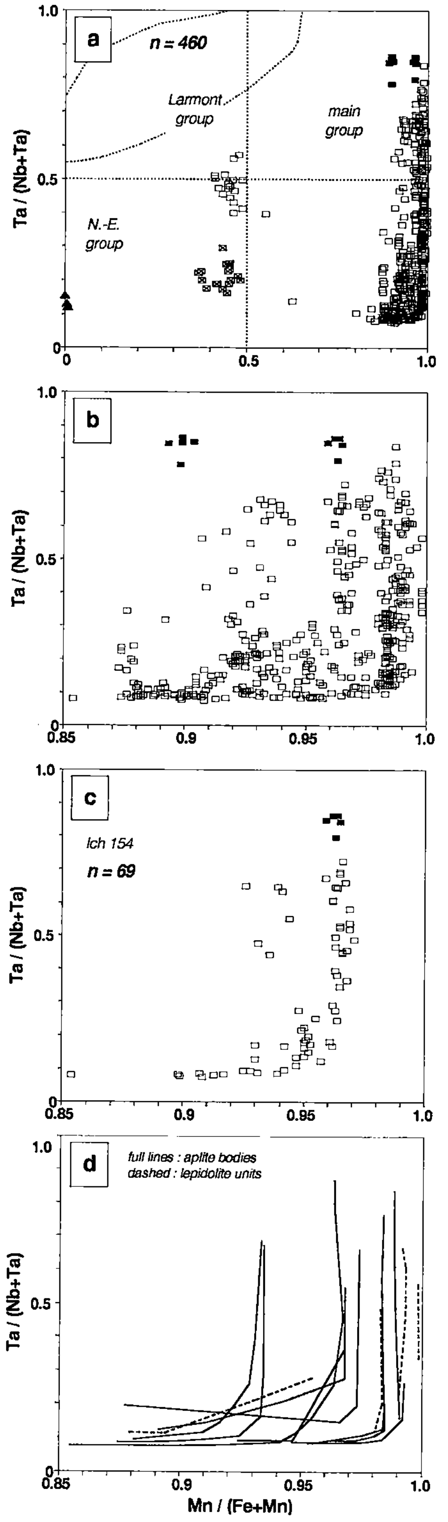

FIG. 6. Columbite – tantalite quadrilateral diagrams for Chèdeville pegmatites. (a) Full extent: open squares, columbite – tantalite; closed squares, ixiolite; crossed squares, tungstenian columbite; triangles, niobian rutile; tantalite – tapiolite gap after Černý *et al.* (1992). (b) Enlargement of the field covered by columbite – tantalite and ixiolite from the Main-group pegmatites. (c) Example of evolution within a single sample; such a pattern is represented in part d by a curve. (d) Summary of columbite – tantalite compositions for all samples from the Main group (aplite and lepidolite units).

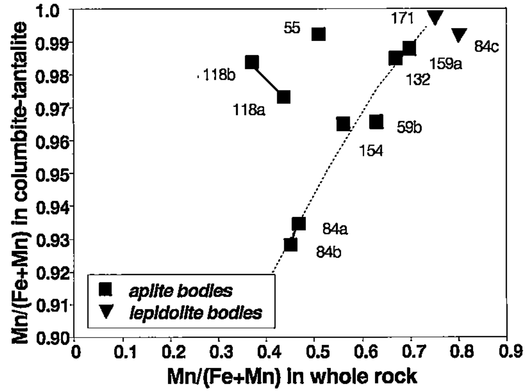

FIG. 7. Relationships between the asymptotic Mn number (X_{Mn}) in columbite – tantalite and the Mn number (X_{Mn}) in the whole rock. Tie-line joins samples from the same body of pegmatite. Dashed line shows the trend of least-altered samples of aplite (see text).

In this model, the asymptotic X_{Mn} values are related to the evolution of the pegmatite-forming melts, and may be a valuable indicator of the structure of the pegmatite field. However, it seems to be easily reset by postmagmatic processes and, thus, is a less robust indicator than the corresponding ratio in the whole rock.

Contents of minor elements Ti, W, Sn, and Sc in columbite – tantalite yield insights into the behavior of these elements during crystallization of the melt. *Scandium* contents (between 0.5 and 1.3 wt% Sc_2O_3) have been detected in only five samples of columbite – tantalite (among 38) from the coarse albite zone. This result is not surprising, as aplite units are strongly depleted in Sc. *Tin* is not abundant, with about 20% of the samples below its detection limit at 0.04 wt% SnO_2, 85% below 0.5 wt%, and a maximum value of 2.78 wt% SnO_2. However, ixiolite with Sn contents between 13.27 and 17.55 wt% SnO_2 is present as a rim enclosing columbite – tantalite or as independent crystals. *Tungsten* is detectable in most samples analyzed. However, tungsten contents are low, as about 60% of the samples of columbite – tantalite contain 0.4–1 wt% WO_3. The highest WO_3 values reach 9.0 wt% in the coarse albite zone, 6.0 wt% in the least evolved aplite bodies, and 4.2 wt% in the most evolved ones. In tungstenian columbite from the Larmont group, WO_3 ranges from 13.15 to 20.44 wt%. *Titanium* is less abundant (in weight) than tungsten, as 75% of samples analyzed contain less than 1 wt% TiO_2, and the highest value is 4.12 wt% TiO_2. On the basis of titanium contents, the compositions can be split into two groups, a regular trend and a set of discordant analyses (Fig. 8).

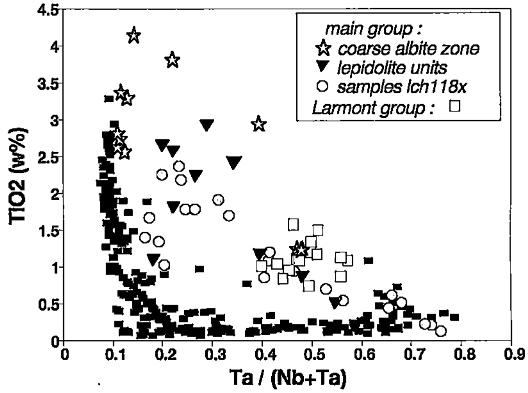

FIG. 8. Evolution of titanium contents in columbite – tantalite. Most samples (solid squares) plot along a well-defined trend; only samples deviating distinctly from this trend have been distinguished.

The main trend is again made up of two parts. In the first part, a steep decrease of TiO_2 contents is anticorrelated with a restricted increase of X_{Ta}, up to approximately 0.23. This part is related to the "horizontal branch" of the evolution in the columbite – tantalite quadrilateral (Fig. 6), and reflects the very usual behavior of Ti in high-silica melts. The second part of the trend is characterized by low, constant or even slightly increasing contents of titanium correlated with large variations of X_{Ta}, suggesting an increase of Ti activity in residual melts produced by crystallization. This effect, although of limited extent, is in agreement with experimental evidence of increased Ti solubility with increasing contents of fluorine in F-rich melts (Keppler 1993).

Discordant samples, with higher Ti contents, belong to specific samples, including the coarse albite zone, lepidolite units, slightly altered samples 118, and the Larmont group, the latter being intrusive within gneisses. The discordant samples attest to the mobility of titanium in hydrothermal fluids.

Evolution along a section through a zoned crystal summarizes the previous observations (Fig. 9). In the following, assignment of features to specific events is done by comparison with the general evolutionary trends described above. The core is characterized by a low X_{Ta}, moderate to low Sn contents, and high W contents. A first zone is characterized by a strong increase of X_{Ta} and Sn content, and by very low W contents. This zone is interpreted as representing the end of the magmatic stage. A second zone has again low X_{Ta} and Sn content. Up to this stage, X_{Mn} remains constant, but finally, at one end of the crystal, a noticeable decrease of X_{Mn} is correlated with a moderate increase in Sn content. During crystallization of the second zone and of the rim, which are both interpreted as hydrothermal, W contents do not vary. This complex pattern of zoning is shown in Figure 10. In the main crystal, the magmatic stage is limited by the highest Ta contents around the Ta-depleted core; a large Ta-poor overgrowth is evident at the right, but much more

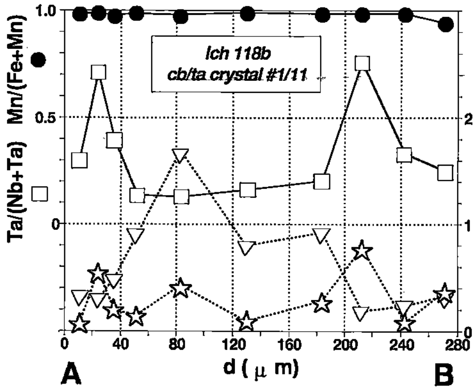

FIG. 9. Ta/Nb and minor-element (W, Sn) zoning in crystal of columbite – tantalite shown in Figure 10 along A–B line, revealing a three-stage growth.

restricted at the left, and the most Ta-poor rim is present at the upper right corner, associated with increased Sn contents.

Microlite group

Microlite *sensu stricto* has been found as a thick overgrowth on columbite – tantalite in the massive lepidolite unit only. The *A* site is saturated with Na and Ca as the only cations, and X_{Ta} (0.83) is higher than in the enclosed columbite – tantalite (0.41).

Uranmicrolite is more common (Table 3), although it occurs as tiny metamict, commonly idiomorphic, crystals. The *B* site is almost exclusively occupied by Nb and Ta atoms, and Ta predominates over Nb, with X_{Ta} ranging from 0.72 to 0.95, most samples analyzed being greater than 0.88. There is a large proportion of vacancies in the *A* site, with an occupancy rate between 15 and 35%. Ca and U are the major cations present in the *A* site (Fig. 11), Fe + Mn account for 10–20% of the site, Ce for 2–4%, Pb for 2–4%, with some analyses showing up to 18% in a sample with K-feldspar development, K for 4–10%, and Na is absent. The population of uranmicrolite is homogeneous, irrespective of the host rock, suggesting that there is a single stage of uranmicrolite crystallization. This implies that uranmicrolite is related to the metasomatic stage of evolution.

Cassiterite

The Nb–Ta contents in cassiterite are variable (Table 4), from 0 to 7.92 wt% Nb_2O_5 and to 12.61 wt% Ta_2O_5, with X_{Ta} evenly distributed between 0.05 and 0.70. In contrast, X_{Mn} values range from 0.20 to 0.95, with two sharp peaks at 0.45 and 0.75. Comparison

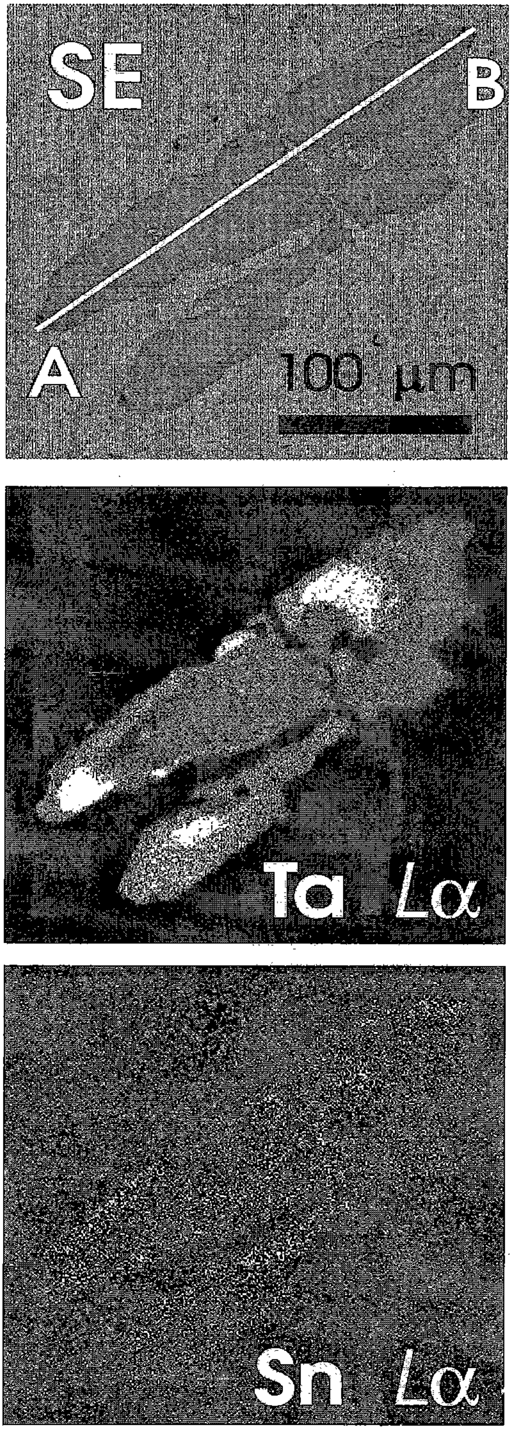

FIG. 10. X-ray image of Ta and Sn in the zoned crystal of columbite – tantalite described in Figure 9 (the A–B profile is represented by the white line on the secondary-electron (SE) image at the top).

TABLE 3. COMPOSITION OF MICROLITE-GROUP MINERALS, CHEDEVILLE, MASSIF CENTRAL

unit	aplite		lep.layer	massive lep.	
sample	—lch118b—		lch159b	——lch171——	
spot #	**5205**	**5210**	**5231**	**433**	**447**
WO_3	0.51	0.39	1.08	0.59	0.32
Nb_2O_5	3.24	2.72	4.34	13.46	8.62
Ta_2O_5	67.78	71.49	68.66	66.22	71.48
TiO_2	0.12		0.04		
SiO_2	4.16	1.16	1.62	0.29	
ThO_2		0.17			
UO_2	10.79	11.43	12.46	10.51	0.24
Ce_2O_3	0.52	1.21	0.50		
FeO	1.02	1.00	0.81	0.39	
MnO	0.08	0.16	0.12		0.28
CaO	0.57	2.46	1.66	0.80	11.46
PbO	3.58	1.00	0.90		
Na_2O					5.83
K_2O	0.28	0.38	0.15	0.25	
F					4.75
total	92.65	93.57	92.34	92.51	100.98
W	0.013	0.010	0.027	0.013	0.007
Nb	0.146	0.118	0.187	0.502	0.333
Ta	1.833	1.872	1.783	1.486	1.660
Ti	0.009		0.003		
Si	0.414	0.112	0.155	0.024	
Th		0.004			
U	0.239	0.245	0.265	0.193	0.005
Ce	0.019	0.043	0.017		
Fe	0.085	0.081	0.065	0.027	
Mn	0.007	0.013	0.010		0.020
Ca	0.058	0.254	0.170	0.071	1.049
Pb	0.096	0.026	0.023		
Na					0.966
K	0.036	0.047	0.018	0.026	
A site	0.540	0.713	0.568	0.317	2.040

Structural formulæ on the basis of 2 (W+Nb+Ta+Ti) atoms per formula unit. A blank indicates values below detection limits: TiO_2, 0.02%; ThO_2, 0.05%; Ce_2O_3, 0.10%; FeO, 0.03%; MnO, 0.03%; PbO, 0.07%; Na_2O, 0.02%; K_2O, 0.01%; F, 0.21%.

with X_{Mn} values in columbite – tantalite shows the preference for Fe in the cassiterite structure over Mn as compared with columbite – tantalite. Mass-balance estimates of the amount of Nb–Ta carried by cassiterite cluster around 10–15% of the total Nb or Ta in the whole rock for most aplite bodies; it may reach up to 20–35% in aplite samples where columbite – tantalite is scarce, or in lepidolite layers between units, and drops to 1–2% in some lepidolite bodies. In contrast to Nb and Ta, Ti and W contents are low.

Charge balance in Nb–Ta-bearing cassiterite usually involves incorporation of Fe and Mn, following the substitution scheme $Sn^{4+}{}_{-3}(Nb,Ta)^{5+}{}_{+2}(Fe,Mn)^{2+}{}_{+1}$. In a (Nb+Ta) *versus* 2(Fe + Mn) diagram (Fig. 12), data points should plot along the diagonal line. This is the case for cassiterite from the northeastern and Larmont groups. However, for each sample from the Main group, cassiterite compositions having significant Nb–Ta contents plot along straight lines with a slope of 1 (a few examples are outlined on the figure). This means that cassiterite crystals have an excess of Nb–Ta with respect to stoichiometry, and that this excess is (1) independent of the Nb–Ta contents in cassiterite, and (2) specific for each sample. Moreover, there is a strong correlation between the excess of Nb–Ta in cassiterite, and the Li contents in the whole rock (inset in Fig. 12). The exceptions to this correlation are metasomatically altered samples, involving either replacement of lepidolite by K-feldspar and concomitant leaching of Li in sample 118b, or strong increase of lepidolite contents and concomitant input of Li in sample 84c. The significance of this trend and of its curved aspect is as yet unclear. Given the small difference between ionic radius of Li^+ (0.82 Å) and Sn^{4+} (0.77 Å) in six-fold coordination (Whittaker & Muntus 1970), the incorporation of Li may ensure charge compensation in Nb–Ta-rich cassiterite formed in Li-rich, Fe–Mn-poor environments.

Zircon and related minerals

As a rule, crystals of zircon are small and rare. In bodies of massive lepidolite, however, zircon may locally be abundant. Its habit is easily identified, by its {111} faces and the lack of {110} faces. The chemical composition (Table 5) is characterized by low totals, possibly indicating a hydrated character, and low Zr/Hf ratio. The proportion of the hafnon end-member, X_{Hf}, varies from 0.04 to 0.12, noticeably higher than 0.03 usually encountered in crustal zircon. In aplite bodies or in layers of lepidolite, some of the analyzed crystals are zoned, with a rim slightly richer in Hf than the core, with X_{Hf} values ranging from 0.058 to 0.085 or 0.042 to 0.069.

In zircon from the main group, U, Ca, Fe, Al, P and Y are enriched, and Sc and, in most cases, Th are depleted. It is noteworthy that, whereas Y and P are usually tied up in zircon according to a $(ZrSi)_{-1}(YP)_1$ xenotime-like scheme of substitution, leading to P/Y atomic ratios not very different from unity, phosphorus and yttrium are independent variables in zircon at Chèdeville, and levels of phosphorus are much higher than required by the $(ZrSi)_{-1}(YP)_1$ substitution. Actually, the P/Y atomic ratio is related to the nature of the host rock. In massive lepidolite units, P/Y ranges from 1 to 3.5, as opposed to 13 to 25 in one crystal of zircon from an aplite unit and two from a lepidolite layer. The two types of lepidolite unit are, therefore, likely to result from different processes, or from similar processes acting in different physical context or on different initial rocks. Finally, high Th values, from 3.15 to 5.11 wt% ThO_2, have been found in zircon from the lepidolite layer.

Overall, the properties of zircon crystals from the Main group are similar to those of the Beauvoir granite, which has a pegmatitic affinity, as noticed by Wang *et al.* (1992a). In contrast, zircon from the Northeastern

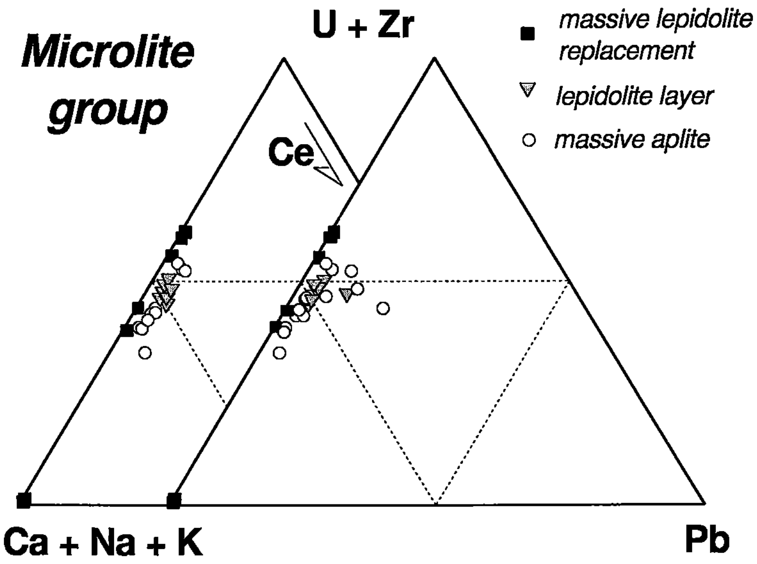

FIG. 11. *A*-site cations in microlite-group minerals. Note that vacancies are not represented on this diagram.

TABLE 4. COMPOSITION OF CASSITERITE, CHEDEVILLE, MASSIF CENTRAL

unit	coarse p.	aplite			lepidolite layer		lepidolite
sample	lch176d	lch118b	lch132	lch175a	lch175b	lch159b	lch84c
spot #	**5883**	**6116**	**6073**	**5982**	**6003**	**5930**	**6158**
SnO_2	93.86	81.26	88.40	91.45	91.93	93.92	87.15
TiO_2	0.16	1.12	1.10			0.25	
Nb_2O_5	0.68	7.92	5.55	2.71	2.05	1.91	1.71
Ta_2O_5	1.42	6.72	3.63	5.05	4.94	2.99	9.01
WO_3	2.46	0.28					
FeO		0.96	0.88	0.41	0.08	0.05	0.21
MnO		2.01	0.75	0.71	0.47	0.51	1.41
total	98.58	100.27	100.31	100.33	99.47	99.63	99.49
Sn	0.951	0.783	0.857	0.907	0.923	0.937	0.881
Ti	0.003	0.020	0.020			0.005	
Nb	0.008	0.087	0.061	0.030	0.023	0.022	0.020
Ta	0.010	0.044	0.024	0.034	0.034	0.020	0.062
W	0.016	0.002					
Fe		0.019	0.018	0.009	0.002	0.001	0.004
Mn		0.041	0.015	0.015	0.010	0.011	0.030
Σcat.	0.988	0.996	0.995	0.995	0.992	0.996	0.997

Structural formulæ on the basis of 2 oxygen atoms per formula unit. A blank indicates values below detection limits: TiO_2, 0.06%; WO_3, 0.05%; FeO, 0.03%; MnO, 0.04%.

group is quite distinct with respect to P/Y, ranging from 4 to 10, and to Th content, which is systematically high. Such zircon is associated with unidentified minerals poor in Zr and rich in Th (up to 17.6 wt% ThO_2), P (up to 20.6 wt% P_2O_5) and Al (up to 6.4 wt% Al_2O_3), and with U–Th-rich monazite (3.07 wt% UO_2, 8.11 wt% ThO_2). This mineral assemblage points out again the differences between the two groups of pegmatite.

Phosphates

The most common primary phosphate species is amblygonite, which is present in each pegmatite zone except in lepidolite layers and in some units of massive lepidolite. Usually, it is the only primary phosphate mineral. However, some samples of the coarse albite zone are rich in large phosphate crystals, which include montebrasite, apatite, and an unidentified, usually

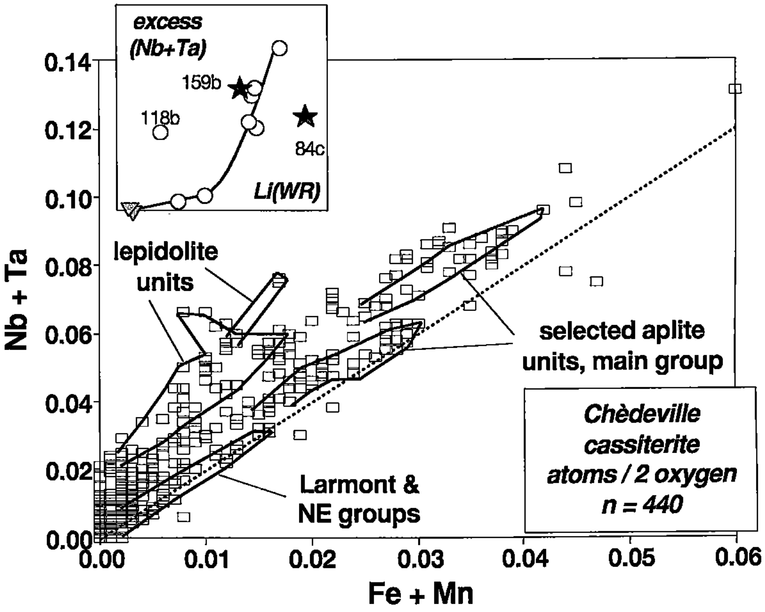

FIG. 12. Evidence for an excess of pentavalent cations Nb–Ta with respect to divalent cations Fe–Mn in cassiterite. The stoichiometric replacement scheme $Sn^{4+}_{-3}(Nb,Ta)^{5+}_{+2}(Fe,Mn)^{2+}_{+1}$ is indicated by the dotted line: crystals from a given sample (some are outlined) usually plot along a line parallel to this "zero" line, allowing one to define a mean excess of (Nb + Ta) in cassiterite, relative to the above substitution scheme. Inset shows that this excess of (Nb + Ta) is correlated with the lithium contents in whole rock (inverted triangles, NE and Larmont groups; circles, aplite units and stars, lepidolite units from the Main group).

strongly altered, aluminum-bearing phosphate. Alteration phases formed after the latter mineral are apatite, and Sr- and Ca-rich members of the goyazite – crandallite series. However, it must be stressed that a complete inventory of phosphates is still to be done.

BULK-ROCK GEOCHEMISTRY

The bulk composition of the pegmatites has been approached through the chemical analysis of aplitic units. Whether or not aplitic parts may be taken as a proxy for whole bodies remains an open question in our case; however, it must be stressed that analyzed samples are devoid of coarse crystals, and that the central aplitic parts are usually free of marginal "stockscheider" which could have trapped elements, so that samples may be considered as representative of a rare-metal-enriched melt (volatile species notwithstanding). It must be remembered, however, that relationships between a bulk pegmatite body and its aplitic unit are not yet precisely constrained, at least in our case, and that this loss of information may result in scatter in the data about trends representative of the processes governing the evolution of pegmatite-forming melts.

Analytical methods include X-ray fluorescence on fused glasses (Si, Al, Ca, K, and P) or on pelleted powders (Ga, Sr, Zr, Nb, Sn, and Pb), inductively coupled plasma – atomic emission spectrometry after acid digestion (Li, Be, Mg, Ti, V, Cu, Y, and Ba), instrumental thermal neutron-activation analyses with irradiation times of 30 s (Na and Mn) and 1 h (Fe, Sc, Cr, Co, Zn, some *REE*, and Hf), and instrumental epithermal neutron-activation analyses (Ni, As, Br, Rb, Mo, Ag, Sb, Cs, some *REE*, Ta, W, Au, Th, and U). Radiochemical neutron-activation analysis with group separation of the rare-earth elements (*REE*) has been used for samples lch59a, lch59b, lch118a, and lch171. A complete description of analytical procedure can be found in Raimbault *et al.* (1995).

Evolution within and between pegmatite bodies

At first glance, compositions of Main-group aplite units seem uniform (Table 6); except for a few elements, the level of most elements is bracketed within

TABLE 5. COMPOSITION OF ZIRCON, CHEDEVILLE, MASSIF CENTRAL

group	main group					NE group	
unit	aplite		lep. layer	massive lepidolite		aplite	
sample	lch84b		lch159b	lch82e	lch171	lch32	
spot #	5519 core	5516 rim	5534	283	279	5509	5512
ZrO_2	48.97	51.61	48.85	56.83	58.53	51.03	41.97
HfO_2	5.94	8.15	5.45	5.70	12.77	4.12	3.00
ThO_2			4.16			4.95	10.87
UO_2	0.94	0.35	3.05	0.91		3.07	2.96
TiO_2					0.43	0.11	
Sc_2O_3						0.24	
Y_2O_3	0.29	0.22	0.24	0.33		0.72	0.65
Al_2O_3	1.49	3.09	5.09	0.71	0.07	1.87	5.41
FeO	2.07	1.18	1.70	0.68		1.45	0.74
CaO	1.02	0.84	0.87	0.66		1.35	2.07
SiO_2	23.23	25.22	17.45	28.61	29.93	23.97	15.96
P_2O_5	2.94	3.38	4.10	0.72	0.15	2.10	11.67
total	86.89	94.04	90.96	95.14	101.87	94.98	95.30
Zr	0.849	0.821	0.845	0.908	0.911	0.841	0.684
Hf	0.060	0.076	0.055	0.053	0.116	0.040	0.029
Th			0.034			0.038	0.083
U	0.007	0.003	0.024	0.007		0.023	0.022
Ti					0.010	0.003	
Sc						0.007	
Y	0.005	0.004	0.005	0.006		0.013	0.012
Al	0.062	0.119	0.213	0.027	0.003	0.075	0.213
Fe	0.062	0.032	0.050	0.019		0.041	0.021
Ca	0.039	0.029	0.033	0.023		0.049	0.074
Si	0.826	0.823	0.619	0.937	0.955	0.810	0.533
P	0.089	0.093	0.123	0.020	0.004	0.060	0.330

Structural formulæ on the basis of 2 cations per formula unit. A blank indicates values below detection limits: ThO_2, 0.04%; UO_2, 0.04%; TiO_2, 0.03%; Sc_2O_3, 0.05%; Y_2O_3, 0.05%; FeO, 0.02%; CaO, 0.01%.

narrow ranges. Some heterogeneity does exist, however, as variation within each facies exceeds that in similar rare-metal-enriched granites (*e.g.*, Beauvoir granite: Raimbault *et al.* 1995).

At several localities in the Main group, two samples of the aplite unit have been collected at different levels in the section of the dykes, or even in two adjacent veins in the same quarry (Table 6, Figs. 2–4). Differences within each pair may be due to different degrees or styles of alteration, for example, in the pair #118, or to sample heterogeneity, for example with regards to the ore elements Sn, Nb and Ta. However, critical parameters such as Zr/Hf, Fe/Mn and Nb/Ta (Fig. 13), and contents of elements such as Rb, Zr, and Ti, point to the intrinsic homogeneity of the aplite unit at a given locality, as was already suggested by the study of asymptotic X_{Mn} values in columbite – tantalite (see the previous section). (The lateral extent of such homogeneous domains is not known, but an evaluation is provided by distribution of samples along the central part of the Main group, shown in Figure 3.)

Such homogeneity suggests that at each locality (*i.e.*, in each pegmatite body, as defined in the previous sections), the composition of a specific batch of magma has been recorded by aplite units. The heterogeneity within the set of available bulk-compositions should therefore probe the evolution of melts within the Main group. Several elements such as Rb or Ta are usually used as monitors of degree of evolution, mainly due to their "hygromagmaphile" character (Raimbault *et al.* 1987). However, whereas Rb is hosted by major mineral phases and therefore evenly distributed in rocks, Ta is carried by sparse ore minerals, the uneven distribution of which leads to erratic variations hiding primary variations in melts, and precluding the use of Ta contents for evaluating evolutionary grades. It is, therefore, necessary to identify additional indicators.

Besides Rb contents, a second indicator of evolution is provided by the "asymptotic X_{Mn}" value in columbite – tantalite, as well as the corresponding Fe/Mn value in the whole rock, both of which have been shown to be useful in this respect (Fig. 7). In addition, Raimbault *et al.* (1995) have shown that zircon is soluble and that Zr is a hygromagmaphile element in highly depolymerized, F-rich melts of the Beauvoir series. Experimental work by Keppler (1993) leads to the same result. As a consequence, Zr contents should increase with degree of evolution of such melts, providing a third indicator. Enrichment of Zr and Hf in Main-group aplites (Fig. 13a) occurs at a constant Zr/Hf, precluding the crystallization of zircon (see a complete discussion in Raimbault *et al.* 1995). This shows that Zr contents can indeed be used to evaluate degree of evolution in Main-group granitic pegmatites at Chèdeville.

Three parameters may thus be used to define an evolutionary sequence within the set of compositions of the Main-group pegmatites: Fe/Mn ratio decreases, whereas both Zr and Rb contents increase with degree of evolution. Examination of the results of chemical analyses (Table 6) therefore provides three sequences of ranked samples, according to the three criteria. As expected for robust estimates of degree of evolution, the three sequences, although of different sensitivity, define a unique evolutionary sequence among the different bodies that make up the Main group: 1) Rb contents increase from *ca.* 1100 ppm at locality #84 to 1200 ppm (#118), 1600 ppm (#59), 1750 ppm (#175), 1900 ppm (#55, 132 and 154) and up to 2200 ppm at locality #159. 2) Zr contents define three clusters, the lowest concentration and therefore least evolved at localities #84–#118 (21–23 ppm), an intermediate level at locality #59 (25–26 ppm), and the highest and most evolved rock at the remaining localities #55, 132, 154, and 159 (30–32 ppm). 3) The Fe/Mn value discriminates between two groups only. The least evolved group, with Fe/Mn > 1, coincides with the least evolved samples determined by the two other parameters.

The evolutionary sequence within the pegmatite population is therefore well defined, despite a very restricted interval of compositions. Only a few elements, Li, Rb, Zr, Hf and, to a lesser extent, W and Ga, are found to increase consistently in concentration with degree of evolution. Although the highest Ta and Nb values are found in the most evolved aplite unit, there is no systematic relationship between degree of evolution and contents of ore elements Nb, Ta, and Sn, which are scattered but retain a constant Nb/Ta ratio (Fig. 13) characteristic of each pegmatite group. Other elements

TABLE 6. WHOLE-ROCK COMPOSITION OF APLITE UNITS, MAIN PEGMATITE GROUP, CHEDEVILLE FIELD, MASSIF CENTRAL

	lch55	lch59a	lch59b	lch84a	lch84b	lch118a	lch118b	lch132	lch154	lch159a	lch175a
SiO_2	67.03	70.52	69.40	66.15	66.46	69.07	69.39	65.06	65.94	66.39	67.49
Al_2O_3	17.58	18.27	18.39	17.88	17.16	18.28	16.73	17.44	17.11	17.45	16.71
Fe_2O_3	0.19	0.11	0.11	0.20	0.17	0.22	0.11	0.10	0.14	0.05	0.07
MnO	0.17	0.15	0.17	0.15	0.13	0.15	0.06	0.19	0.16	0.11	0.08
CaO	0.19	0.16	0.14	0.60	0.11	0.30	0.22	0.48	0.64	0.34	0.23
Na_2O	3.95	3.73	5.62	5.15	5.05	6.07	4.23	4.15	3.80	3.99	4.24
K_2O	3.25	2.61	2.54	2.47	2.66	2.26	4.70	3.35	3.09	3.48	3.01
P_2O_5	0.98	0.85	0.79	0.76	0.30	0.86	0.27	1.37	1.05	0.57	0.81
LoI	2.82	2.13	2.07	2.85	2.97	1.85	1.96	2.72	3.35	2.90	2.55
total	96.16	98.53	99.23	96.21	95.01	99.06	97.67	94.86	95.28	95.28	95.19
Li	6025			3750	2671		1813	5819	5627	6912	5903
Be	269			262	189		201	202	242	241	218
Mg	48			98	123		168	30	44	70	65
Sc (ppb)	99.7	143	156	372	220	129	242	136	417	166	157
Ti	81	74	54	103	105	60	54	150	104	94	49
V	0.3			0.2	0.1		0.7	0.7	0.3	0.9	0.3
Cr	<0.4			<0.3	<0.4		<0.6	<0.4	<0.4	<0.8	<0.5
Mn	1327	1163	1284	1189	975	1180	444	1438	1255	872	652
Fe	1300	760	770	1370	1190	1530	758	715	998	381	496
Co (ppb)	101	29	68	1081	425	38	210	60	311	240	66
Ni	<8			<9	<7		<6	<5	<10	<13	<5
Cu	3.4			5.7	3.4		7.4	3.9	2.9	4.4	3.8
Zn	75.2	99.0	109.0	131.6	98.5	147.4	15.4	104.3	100.5	43.0	34.6
Ga	44.1	36.7	37.0	37.4	35.0	32.6	32.6	42.9	38.0	44.3	35.1
As	2.54	2.5	2.7	10.7	5.9	5.1	1.92	4.13	5.2	1.50	2.9
Br	0.61	<1	1.7	2.3	3.5	1.0	<0.9	<0.6	1.9	<1	0.62
Rb	1870	1584	1639	1095	1097	1186	1232	1951	1954	2166	1751
Sr	76.8	52.0	57.8	69.4	16.1	151.1	28.9	538	429	54.6	59.6
Y	1.4			2.39	0.84		0.88	0.30	2.37	0.42	0.31
Zr	30.7	26.0	25.2	23.6	21.8	21.0	32.5	26.6	31.6	30.6	29.9
Nb	58.5	76.1	73.4	82.2	53.3	43.2	97.4	66.4	70.8	130.5	50.5
Mo	<1.1	1.3	2.0	1.2	<1.2	<1.3	<1.7	<1.3	1.8	<1.8	1.8
Ag	<0.5	<0.4	<0.4	<0.5	<0.4	<0.3	<0.4	<0.3	0.31	<0.7	0.39
Sn	476	657	1077	685	392	343	581	577	737	715	462
Sb (ppb)	160	110	154	102	65	51	159	43	148	67	93
Cs	170	245	242	119.8	84.6	111.7	107.2	177	246	298	298
Ba	26			48	2	367	6	18	680	43	10
La	0.64	0.158	0.759	1.75	0.66	0.126	1.09	0.32	2.36	0.90	0.69
Ce	1.35	0.359	1.51	2.66	0.87	0.322	1.53	0.61	4.21	1.58	1.40
Sm (ppb)	65	24.0	125	397	124	79.6	85	82	402		105
Eu (ppb)	14.5	4.4	21.8	114	42.4	14.4	16.8	6.9	108	17.7	15.0
Tb (ppb)	<70	6.3	25.3	115	35	14.2		11	106		
Yb (ppb)	96	22.1	33.1	230	55	74.4		44	164		
Lu (ppb)	17	3.8	4.3	29	11	12.1	19	8	22	<22	
Hf	1.49	1.42	1.46	1.27	1.19	1.06	1.93	0.86	1.65	1.56	1.72
Ta	93.3	115.6	98.8	103.2	87.3	88.3	161	79.2	136	185	68.8
W	17.9	19.6	23.4	16.7	14.4	17.1	8.2	22.3	18.2	23.6	17.5
Au (ppb)	<3	<4	<4	<3	<3	<3	<4	<3	<5	<4	<4
Pb	9.8	17.1	27.1	13.3	12.2	15.3	16.8	10.2	8.6	14.3	11.2
Th	1.07	1.92	2.41	2.27	1.23	1.60	2.03	0.86	1.28	2.06	1.48
U	11.50	2.73	2.41	5.71	3.37	5.41	9.15	5.03	11.5	6.00	4.76

Major elements in %, trace elements in ppm unless specified. Blank: not analyzed.
Digits in sample designation refer to outcrop numbers (Fig. 2 to 3).

have more or less constant values, except Sr, As, and Ba, which display an erratic behavior. The presence of goyazite as a low-temperature alteration mineral may explain the mobility of Sr. However, it must be emphasized that the enclosing leucogranites are Sr-poor and thus unlikely sources of Sr, and that Sr isotope geochemistry has shown that high Sr contents in the Beauvoir granite are an intrinsic property of the melts (Raimbault *et al.* 1995).

In general, the least-evolved samples are located in the central part of the Main group, whereas the most evolved ones are located at the southwestern edge (Figs. 2, 3). However, some localities in the central part of the pegmatite group exhibit very evolved characteristics as well (#132), arguing again for the multiple intrusion model derived from field studies. The Larmont group, part of the same alignment as the Main group, seems to be a less evolved member of the

Chèdeville pegmatites, as shown by similar whole-rock Nb/Ta values. The northeastern group has very different chemical (as well as petrographic) characteristics and must be assigned to another family of granitic pegmatites.

Metasomatic processes

In lepidolite units resulting from metasomatic processes, the ratios Zr/Hf, Nb/Ta and Fe/Mn have different values than in the aplite units from which they were derived (Fig. 13, Table 7). Zirconium and hafnium are well correlated in aplite samples with a constant Zr/Hf (Fig. 13a), in contrast with the Beauvoir granite, in which important mobility of Hf has been observed and interpreted as resulting from hydrothermal transfer induced by melt degassing as bubbles rise in the crystallizing magma (Raimbault *et al.* 1995, Candela 1991). The absence of this phenomenon at Chèdeville shows *a contrario* that the chemical composition of aplite units is representative of the chemistry of melts. The only exception is sample #118b, in which replacement of lepidolite by K-feldspar resulted in a leaching of the corresponding elements Li, Fe, Mn, Zn, and W. This justifies *a posteriori* the choice of aplite samples as proxies for rare-metal melts and emphasizes the interest of Chèdeville pegmatites, in which magmatic and hydrothermal stages are better separated than in larger rare-metal-enriched granites, where the latter stages are superimposed onto the former ones.

The geochemical data for two massive lepidolite units and two lepidolite layers are compared to the composition of associated aplite units in Figure 14. The lepidolite layers are located a few cm away from the roof of the vein ("top" layer) and at the contact between massive aplite and banded aplite units ("middle" layer), respectively. The enrichment or depletion patterns of lepidolite units with respect to aplite bodies differ in the two types of lepidolite bodies, and depending on the group of elements considered. A common behavior in all types of lepidolite bodies is observed for the group Ga–Rb–Cs, likely because of the presence of these elements in lepidolite. In contrast, the group of +4 cations Ti–Zr–Hf–Th distinguishes the middle lepidolite layer from all other bodies of lepidolite, the group Sc–Zn–Pb distinguishes layers of lepidolite from massive lepidolite units, and the group of ore elements Sn–Nb–Ta–W–U also distinguishes the middle lepidolite layer from other units of lepidolite, but subdivides the latter subgroup by contrasting the

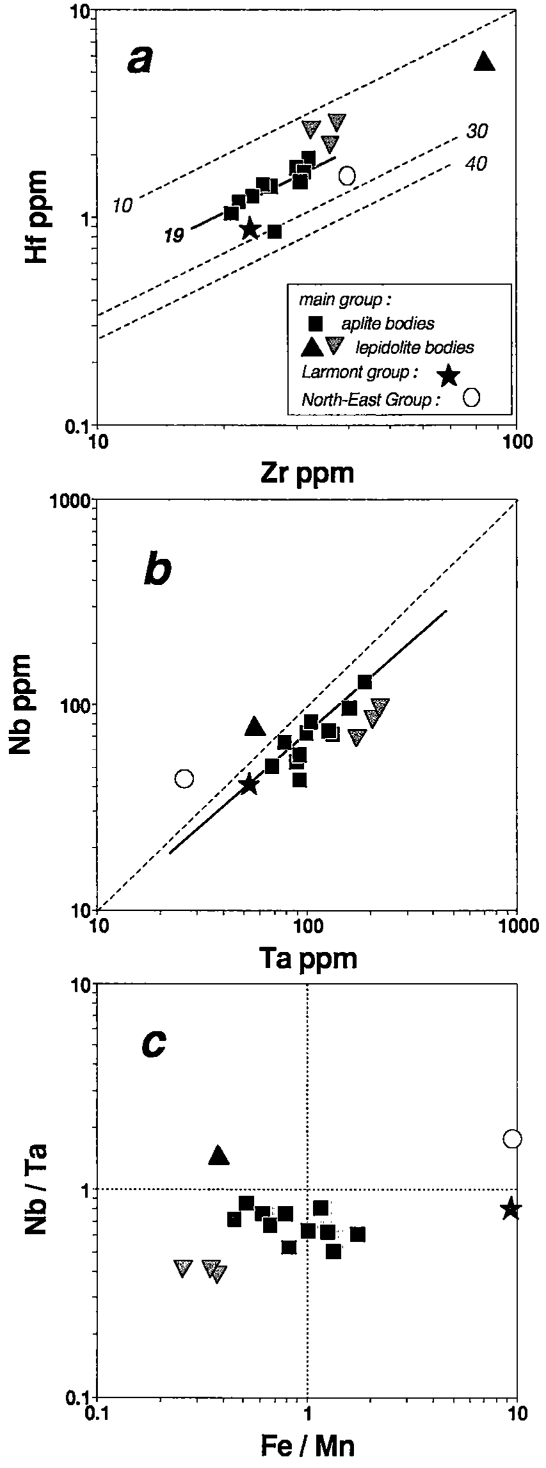

FIG. 13. Chemical evolution in aplite units of Chèdeville pegmatites. (a) Hf *versus* Zr; (b) Nb *versus* Ta; (c) Nb/Ta *versus* Fe/Mn. In (a) and (b), solid lines indicate the evolutionary trends in Main-group aplites, and dashed lines refer to constant Zr/Hf and Nb/Ta values. Grey squares in (c) join pairs of samples from the same locality.

TABLE 7. WHOLE-ROCK COMPOSITION OF LEPIDOLITE UNITS, MAIN PEGMATITE GROUP, AND OF APLITE UNITS, NORTHEASTERN AND LARMONT GROUPS, CHEDEVILLE FIELD, MASSIF CENTRAL

	main group				NE group	Larmont
	massive lepidolite		lepidolite layer		aplite units	
	lch84c	lch171	lch175b	lch159b	lch32	lch178
SiO_2	68.28	69.28	64.18	66.38	71.97	68.13
Al_2O_3	17.40	18.12	18.79	17.29	14.98	17.46
Fe_2O_3	0.06	0.02	0.06	0.06	0.42	0.61
MnO	0.23	0.05	0.15	0.16	0.04	0.06
CaO	0.15	0.13	0.16	0.13	0.28	0.29
Na_2O	0.57	2.02	0.93	0.75	6.28	7.32
K_2O	5.90	4.51	6.10	5.56	1.20	1.60
P_2O_5	0.13	0.85	0.26	0.33	0.32	0.36
LoI	3.26	3.11	4.18	3.73	1.35	1.46
total	95.98	98.09	94.81	94.39	96.84	97.29
Li	8093			5235	878	571
Be	244			401	216	83.1
Mg	186			100	347	154
Sc (ppb)	46	6.9	96	90	528	318
Ti	52	17	175	45	239	94
V	3.4			3.3	1.2	0.6
Cr	<0.9		<2	<1.3	1.17	<0.3
Mn	1740	388	1161	1228	316	472
Fe	432	130	424	441	2940	4230
Co (ppb)	134	<30	112	478	493	247
Ni	<14		<7	<10	<2	<3
Cu	8.5			6.9	2.6	1.6
Zn	44.0	8.7	20.4	20.9	81.9	93.2
Ga	47.5	41.0	53.5	50.0	29.2	31.9
As	1.88	2.5	2.4	0.86	0.51	1.03
Br	<1.2	<1.7	<0.9	1.7	1.43	1.9
Rb	3209	3431	4897	3744	367	441
Sr	13.4	30.3	41.3	97.5	33.2	28.9
Y	2.72			1.71	1.92	0.86
Zr	37.8	32.6	85.0	36.4	39.6	23.5
Nb	98.2	88.4	79.0	71.1	44.3	42.0
Mo	<2.2	<3.4	<2	<3.3	<0.3	<0.9
Ag	0.75	<0.7	0.86	<0.6	0.09	0.13
Sn	389	414	692	200	533	117
Sb (ppb)	<90	65	152	35	47	60
Cs	306	661	1126	487	26.8	77.1
Ba	7			45	17	14
La	0.72	0.241			4.40	1.46
Ce	1.39	0.73			7.54	1.74
Sm (ppb)		54			909	200
Eu (ppb)	<9	13.4			143	44.1
Tb (ppb)		9.8			108	20
Yb (ppb)		26.9			169	128
Lu (ppb)	<20	4.0			26	12
Hf	2.87	2.67	5.68	2.28	1.59	0.88
Ta	234	214	54.7	184	25.6	52.0
W	23.9	21.0	52.5	25.9	7.5	12.1
Au (ppb)	<5	<8	<6	<8	<2	<2
Pb	<3	7.0	<3	8.9	12.3	18.3
Th	2.17	2.19	6.15	1.55	5.35	1.29
U	13.0	14.9	8.75	20.8	4.40	1.82

Major elements in %, trace elements in ppm unless specified.
Blank: not analyzed.

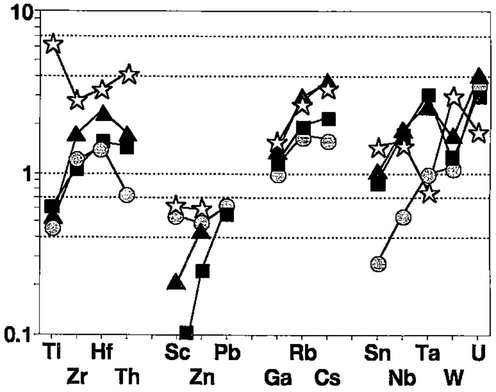

FIG. 14. Ratios of selected trace-element contents in lepidolite bodies to contents in adjacent aplite bodies considered as representative of starting material. Triangles, massive lepidolite body lch84c/aplite lch84a; squares, massive lepidolite body lch171/aplite lch175a; stars, layer between two aplite bodies lch175b/aplite lch175a; circles, layer at the roof of the pegmatite lch159b/aplite lch159a.

top lepidolite layer with the massive lepidolite units (Fig. 14). The trace-element contents of lepidolite units therefore suggest different physical or chemical conditions occurring during the metasomatic processes. A precise assignment of such parameters, *e.g.*, the role of initial composition, or whether the body results from the interaction of fluids with a completely crystallized rock or with a still partly liquid portion of the pegmatite, is beyond the scope of this study.

Ore elements are most commonly enriched, and the metasomatic lepidolite units are the richest ores of Ta and Li, whereas Fe, Sc, Zn are leached during the metasomatic changes leading to the formation of lepidolite units. The most noteworthy feature, however, is the pronounced mobility of elements Ti, Zr, Hf, and Th in sodic, F-rich fluids; these elements are considered immobile in granitic rocks. The mobility of +4 cations in F-rich fluids has also been documented at Echassières by Raimbault *et al.* (1995) and at Suzhou by Charoy & Raimbault (1994).

The Chèdeville pegmatites as products of a rare-metal-enriched melt

The major-element composition of Chèdeville pegmatites must be discussed in the system Si–P–Al–Na–K–Li–O–F. The presence of elements F, Li, P, or a subset of them, has long been noticed in rare-metal-bearing granites. Experimental work (Manning 1981, Martin 1983, London *et al.* 1993) provides the theoretical framework for an explanation of the unusual characteristics of the melts. Low silica and high Al contents, and predominance of Na over K, result from the high abundance of fluxing agents F, P, and Li, which contribute to depolymerize the melt, to lower solidus temperatures, and to replace the eutectic of the Qz–Ab–Or system with cotectic lines in the complex system.

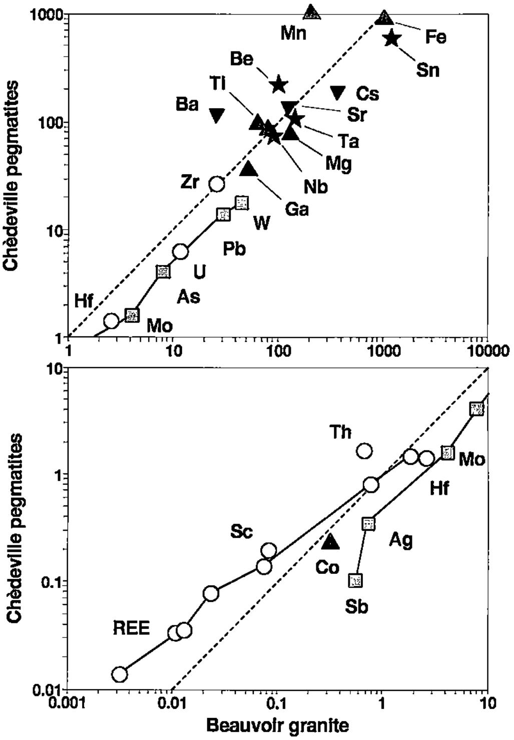

FIG. 15. Trace-element contents in a "composite" aplite unit of Chèdeville pegmatites as compared to B1, the most evolved facies in the Beauvoir rare-metal-enriched granite; Rb and Li are plotted along the line just above the diagram. Squares, chalcophile elements; circles, high-field-strength and rare-earth elements; stars, ore elements; triangles, iron-group transition elements; inverted triangles, alkalies and alkaline-earth elements. All data in ppm; Chèdeville data, mean composition deduced from Table 6, Beauvoir data after Raimbault *et al.* (1995).

The Beauvoir granite is a typical Li–F–P-bearing rare-metal granite that has been studied in detail. The granite is geochemically well defined owing to a large number of analyses (Raimbault *et al.* 1995), and it can be used as a reference material for the comparative study of rare-metal granites. Mean trace-element contents in Chèdeville pegmatites are plotted in Figure 15 against contents in B1, the most evolved facies of the Beauvoir granite. The distance to the first bissectrix of the axes is related to the difference between the two occurrences: the distance remains within ratios less than 5 and rarely larger than 3, despite the unusual

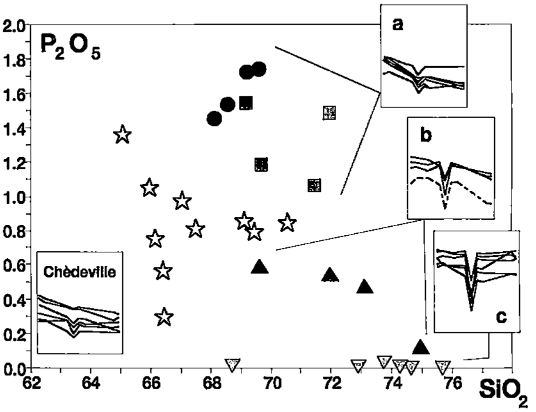

FIG. 16. Phosphorus – silica – *REE* plot for peraluminous rare-metal-enriched or topaz-bearing melts [data from Raimbault *et al.* (1995) and references therein]. Stars, Chèdeville pegmatites, Main group, samples devoid of major metasomatic alteration; circles, very-high-P granites of the Beauvoir B series; squares, other very high-P granites and rhyolite (Beauvoir B' series, Montebras, Argemella, and Richemont); triangles, high- to moderate-P granites (Yichun, Les Châtelliers, Homolka, and East Kemptville); inverted triangles, low-P granites (Cinovec, Shizhuyuan, Ahelehedj, Chavance, Orlovka, and Ary-Bulak). Insets, *REE* chondrite-normalized patterns for Chèdeville pegmatites, and for (a) very high-P melts, (b) high- to moderate-P melts (dashed line is Yichun), (c) low-P melts. The vertical axis of *REE* plots has the same range in all insets.

composition of the Beauvoir granite. Elements that have nearly identical values include Fe–Co–Zn, Ti–Zr–Nb–Ta, Sr, and the light *REE*, whereas Be, Mn, Th, Sc and the heavy *REE* are distinctly more concentrated in the Chèdeville pegmatites, and Sn, Cs, U, the chalcophile elements, and Hf are enriched in Beauvoir granite. Similar degrees of evolution in the two occurrences account for elements that have nearly equal values, although slight differences, such as in Zr/Hf, point to slightly less evolved characteristics in Chèdeville. Other differences may be related to slight differences either during evolution or due to initial conditions; it is worth noting that the Yichun rare-metal-enriched granite, in China, shares its enrichment and depletion patterns with the Chèdeville pegmatites, more so than with the Beauvoir granite (Raimbault, in prep.).

Comparative geochemistry of rare-metal granites has led Raimbault *et al.* (1991) and Taylor (1992) to define high-P and low-P series, the differences being well illustrated in Figure 16. As compared with the flat, sea-gull-like *REE* patterns of low-P series, *REE* patterns of high-P series are characterized by low to very low *REE* contents, variable fractionation, and moderate Eu anomalies. These low values are the result of the low solubility of monazite in peraluminous melts (Rapp & Watson 1986) and increased activity of phosphorus. Phosphorus contents in the Chèdeville pegmatites are lower than in the most P-rich granites, and are comparable to P contents in the Yichun granite (Yin *et al.* 1995). In addition, trace-element patterns at Chèdeville and Yichun are similar and differ slightly from those in the Beauvoir granite. This finding suggests a major influence of phosphorus on the behavior of some trace elements, leading to a gradation of geochemical properties from intermediate-P to very high-P suites within the high-P series of rare-metal-enriched granites. However, in detail the *REE* patterns of the Chèdeville pegmatites are more comparable to those of very high-P granites than to those for the Yichun granite (unpubl. data). Although the link is not clear at present, it is tempting to correlate this phenomenon with the differences in alumina saturation Al/(Na + K), which is lower in the latter (about 1.4 in Yichun granite) than in the former group (about 1.5 in Beauvoir granite and 1.67 ± 0.17 in the Chèdeville pegmatites).

Undoubtedly, the Chèdeville pegmatites belong to the high-P type of rare-metal-enriched granites, but subtle differences exist within the family of peraluminous rare-metal-enriched granites, owing to the progressive involvement of elements affecting the structure of melts: Li–F enrichment is common to all occurrences, P contents separate high-P and low-P series, and excess alumina further subdivides the series. The range of geochemical variation observed in Chèdeville pegmatites is too narrow to allow for a detailed discussion of genetic models. However, parameters like low Zr/Hf value, and comparison with very similar well-constrained occurrences (*e.g.*, Yin *et al.* 1995, Černý & Lenton 1995, Raimbault *et al.* 1995) strongly argue for a fractional-crystallization-like model.

CONCLUSIONS

Mineralogy of the Chèdeville pegmatites and patterns of columbite – tantalite evolution point out an affiliation to the rare-element-enriched class, complex type, lepidolite subtype of granitic pegmatite in the classification of Černý (1989), with unusually high phosphate contents.

Whole-rock geochemistry of aplitic units show an extreme enrichment in Li–Rb–Cs–Ta–Sn, in agreement with the LCT family of Černý (1992). In classifications of rare-metal-bearing peraluminous granites (Raimbault *et al.* 1991, Taylor 1992), the Chèdeville pegmatites belong to the high-P type, and detailed comparison with other granites of this type indicates complex geochemical gradations in melts in correlation with variations of phosphorus contents and aluminum saturation.

The preferred model for emplacement of pegmatites, as deduced from field, mineralogical, and geochemical studies, involves multiple intrusions of successive melts, probably derived by fractional crystallization from a hidden source, in a swarm of small vein-like spaces created by pull-apart tectonics in a shallow environment. A magmatic origin for the rare-metal enrichment is indicated by aplite units, well separated from metasomatic lepidolite units, which account for *ca.* 5% of the pegmatite bodies. Mobility of Th, Zr, Hf in unmixed hydrothermal fluids is related to high Na–F contents in the melt.

ACKNOWLEDGEMENTS

Field work was supported by A.T.P. "Métallogénie" of the Centre National de la Recherche Scientifique. Thanks are due to Jean-Louis Joron for his assistance during analytical work, to Gabriel Raulo for providing first-class thin sections, and to Marie-Claude Forette for performing numerous electron-microprobe analyses. XRF and ICP–AES analyses have been performed at the SPIN department, Ecole des Mines de Saint Etienne, by Jean-Jacques Gruffat and Jacques Moutte. I am also much indebted to Skip Simmons for his encouragements to write this paper, and to Sarah Hanson, Al Falster, and Robert F. Martin for their critical and careful reading of the manuscript.

REFERENCES

Burnol, L. (1974): Granites acides du Nord-Ouest du Massif Central Français et minéralisations associées. IGCP-MAWAM Symposium (Karlovy Vary), 113 p.

Candela, P.A. (1991): Physics of aqueous phase evolution in plutonic environments. *Am. Mineral.* **76**, 1081-1091.

Černý, P. (1982): Anatomy and classification of granitic pegmatites. *In* Granitic Pegmatites in Science and Industry (P. Černý, ed.). *Mineral. Assoc. Can., Short-Course Handbook* **8**, 1-39.

________ (1989): Characteristics of pegmatite deposits of tantalum. *In* Lanthanides, Tantalum and Niobium (P. Möller, P. Černý & F. Saupé, eds.). Springer-Verlag, Berlin, Germany (195-239).

________ (1992): Geochemical and petrogenetic features of mineralization in rare-element granitic pegmatites in the light of current research. *Appl. Geochem.* **7**, 393-416.

________, Ercit, T.S. & Wise, M.A. (1992): The tantalite-tapiolite gap: natural assemblages versus experimental data. *Can. Mineral.* **30**, 587-596.

________ & Lenton, P.G. (1995): The Buck and Pegli lithium deposits, southeastern Manitoba: the problem of updip fractionation in subhorizontal pegmatite sheets. *Econ. Geol.* **90**, 658-675.

Chantraine, J., Burnol, L., Marquaire, C., Geffroy, J., Flageollet, J.-C. & Guyonnaud, G. (1974a): Notice de la carte géologique de la France (1/50000), feuille Ambazac (664). B.R.G.M., Orléans, France.

________, Lajoinie, J.-P. & Autran, A. (1974b): Carte géologique de la France (1/50000), feuille Ambazac (664). B.R.G.M., Orléans, France.

Charoy, B. & Noronha, F. (1996): Multistage growth of a rare-element, volatile-rich microgranite at Argemela (Portugal). *J. Petrol.* **37**, 73-94.

________ & Raimbault, L. (1994): Zr-, Th-, and REE-rich biotite differentiates in the A-type granite pluton of Suzhou (eastern China): the key role of fluorine. *J. Petrol.* **35**, 919-962.

Cheilletz, A., Archibald, D.A., Cuney, M. & Charoy, B. (1992): Ages ^{40}Ar/^{39}Ar du leucogranite à topaze – lépidolite de Beauvoir et des pegmatites sodolithiques de Chèdeville (Nord du Massif Central, France). Signification pétrologique et géodynamique. *C.R. Acad. Sci. Paris* **315**, 326-336.

Cuney, M. & Raimbault, L. (1991): Variscan rare-metal granites and associated mineralizations from the North French Massif Central. *SGA 25th Anniv. Meeting (Nancy), Field Trip Guidebook.*

Duthou, J.-L., Cantagrel, J.-M., Didier, J. & Vialette, Y. (1984): Palaeozoic granitoids from the French Massif Central: age and origin studied by ^{87}Rb–^{87}Sr system. *Phys. Earth Planet. Int.* **35**, 131- 144.

Foord, E.E. (1976): *Mineralogy and Petrogenesis of Layered Pegmatite – Aplite Dikes in the Mesa Grande District, San Diego County, California.* Ph.D. thesis, Stanford Univ., Stanford, California.

Holliger, P., Cuney, M., Friedrich, M. & Turpin, L. (1986): Age carbonifère de l'unité de Brame du complexe granitique peralumineux de Saint-Sylvestre (N.O. Massif Central) défini par les données isotopiques U–Pb sur zircon et monazite. *C.R. Acad. Sci. Paris* **303**, 1309-1312.

Keppler, H. (1993): Influence of fluorine on the enrichment of high field strength trace elements in granitic rocks. *Contrib. Mineral. Petrol.* **114**, 479-488.

Lacroix, A. (1893): *Minéralogie de la France* I. Librairie Polytechnique, Paris, France.

________ (1901): *Minéralogie de la France* III. Librairie Polytechnique, Paris, France.

________ (1910): *Minéralogie de la France* IV. Librairie Polytechnique, Paris, France.

Lentz, D.R. (1997): The phosphorus-enriched, S-type Middle River rhyolite, Tetagouche Group, northeastern New Brunswick. *Can. Mineral.* **35**, 673-690.

London, D. (1984): Experimental phase equilibria in the system $LiAlSiO_4$–SiO_2–H_2O: a petrogenetic grid for lithium-rich pegmatites. *Am. Mineral.* **69**, 995-1004.

________ (1992): The application of experimental petrology to the genesis and crystallization of granitic pegmatites. *Can. Mineral.* **30**, 499-540.

________, ČERNÝ, P., LOOMIS, J.L. & PAN, J.J. (1990): Phosphorus in alkali feldspars of rare-element granitic pegmatites. *Can. Mineral.* **28**, 771-786.

________, MORGAN, G.B., VI, BABB, H.A. & LOOMIS, J.L. (1993): Behaviour and effect of phosphorus in the system Na_2O–K_2O–Al_2O_3–SiO_2–P_2O_5–H_2O at 200 MPa (H_2O). *Contrib. Mineral. Petrol.* **113**, 450-465.

MANNING, D.A.C. (1981): The effect of fluorine on liquidus phase relationships in the system Qz–Ab–Or with excess water at 1 kb. *Contrib. Mineral. Petrol.* **76**, 206-215.

MARTIN, J.S. (1983): An experimental study of the effects of lithium on the granitic system. *Proc. Ussher Soc.* **5**, 417-420.

RAIMBAULT, L. & BURNOL, L. (1998): The Richemont rhyolitic dyke, Massif Central, France: a subvolcanic equivalent of rare-metal granites. *Can. Mineral.* **36**, 265-282.

________, CHAROY, B., CUNEY, M. & POLLARD, P.J. (1991): Comparative geochemistry of Ta- bearing granites. *In* Source, Transport and Deposition of Metals (Pagel, M. & Leroy, J., eds). Balkema, Rotterdam, The Netherlands (793-796).

________, CUNEY, M., AZENCOTT, C., DUTHOU, J.-L. & JORON, J.-L. (1995): Geochemical evidence for a multistage magmatic genesis of Ta–Sn–Li mineralization in the granite at Beauvoir, French Massif Central. *Econ. Geol.* **90**, 548-576.

________, MEYER, G. & TREUIL, M. (1987): Comportements différenciés de W, Sn, U, Ta, Nb dans quelques complexes granitiques du Massif Central Français. *Bull. Minéral.* **110**, 591-601.

RAPP, R.P. & WATSON, E.B. (1986): Monazite solubility and dissolution kinetics: implications for the thorium and light rare earth chemistry of felsic magmas. *Contrib. Mineral. Petrol.* **94**, 304-316.

SARCIA, J.A. (1957): Les gîtes lithinifères du S.-E. des Monts d'Ambazac. *Mines et Métallurgie*, 723- 728.

SUWIMONPRECHA, P., ČERNÝ, P. & FRIEDRICH, G. (1995): Rare metal mineralization related to granites and pegmatites, Phuket, Thailand. *Econ. Geol.* **90**, 603-615.

TAYLOR, R.P. (1992): Petrological and geochemical characteristics of the Pleasant Ridge zinnwaldite – topaz granite, southern New Brunswick, and comparisons with other topaz-bearing felsic rocks. *Can. Mineral.* **30**, 895-921.

WANG, RU CHENG, FONTAN, F. & MONCHOUX, P. (1992a): Disseminated minerals as indicators of the pegmatitic character of Beauvoir granite from Echassières Massif (Allier, France). *Can. Mineral.* **30**, 763-770.

________, ________, ________ & ROSSI, P. (1992b): Recherche des phases porteuses du béryllium dans le granite de Beauvoir (Allier) par analyses chimiques de fractions densimétriques. *C.R. Acad. Sci. Paris* **314**, 671-674.

WHITTAKER, E.J.W. & MUNTUS, R. (1970): Ionic radii for use in geochemistry. *Geochim. Cosmochim. Acta* **34**, 945-956.

YIN, LIN, POLLARD, P.J., HU, SHOUXI & TAYLOR, R.G. (1995): Geologic and geochemical characteristics of the Yichun Ta–Nb–Li deposit, Jiangxi Province, South China. *Econ. Geol.* **90**, 577-585.

Received December 22, 1996, revised manuscript accepted December 15, 1997.